

# Ultrafast laser spectroscopic study on photochromic cycloreversion dynamics in fulgide derivatives: one-photon and multiphoton-gated reactions

Yukihide Ishibashi,<sup>ab</sup> Tetsuro Katayama,<sup>a</sup> Chikashi Ota,<sup>a</sup> Seiya Kobatake,<sup>c</sup> Masahiro Irie,<sup>d</sup> Yasushi Yokoyama<sup>e</sup> and Hiroshi Miyasaka<sup>\*ab</sup>

Received (in Montpellier, France) 16th January 2009, Accepted 24th March 2009

First published as an Advance Article on the web 16th April 2009

DOI: 10.1039/b900999j

Cycloreversion processes of three photochromic fulgide derivatives in toluene solution were investigated by means of picosecond and femtosecond laser photolysis methods. Femtosecond laser irradiation revealed that the cycloreversion processes upon visible one-photon excitation took place within a few ps in these three derivatives. On the other hand, drastic enhancements of the reaction yield were observed under picosecond laser exposure. Excitation intensity effect of the reaction yield and dynamic behaviors revealed that the successive two-photon absorption process leading to higher excited states opened the efficient cycloreversion channel in the three derivatives. The reaction yields in higher excited states were found to be quite large in these three systems, 0.35–0.55, while those in the S<sub>1</sub> state were 0.048–0.21. The correlation of the reaction yield in the S<sub>1</sub> state with that in S<sub>n</sub> states suggest the character of the electronic states connected by the optical absorption plays an important role in the control of the cycloreversion reaction.

## Introduction

Photochromism is a photoinduced reversible isomerization in a chemical species between two forms with different colors. The quick change of molecular properties *via* the photo-induced chemical-bond reconstruction has been attracting much attention from the viewpoints of the fundamental chemical reaction processes and the application to optoelectronic devices.<sup>1–17</sup>

Among various photochromic molecules, diarylethene<sup>3,4</sup> and fulgide<sup>5,6</sup> derivatives undergo cyclization and cycloreversion reactions in 6 $\pi$ -electrocyclic systems in ultrafast time scale.<sup>18–33</sup> Both isomers in the photochromic reactions are thermally stable at the room temperature and different from each other not only in their absorption spectra, but also in various physical and chemical properties such as fluorescence spectra,<sup>11</sup> refractive indices,<sup>12</sup> oxidation/reduction potentials,<sup>13</sup> and chiral properties.<sup>14</sup> In addition, the photochromic reaction can take place even in the crystalline phase.<sup>15–17</sup> These features in fulgide and diarylethene derivatives have been attracting much attention as most promising for applications such as rewritable optical memory and switches.

From the viewpoint of the application, the photochromic systems for actual utilization require several conditions such as (a) thermal stability, (b) high durability, (c) rapid response, (d) high sensitivity, and (e) non-destructive readout capability. Since the reaction in the excited state occurs in competition with other processes in a finite lifetime, a fast rate of the photochromic reaction (rapid response) is of crucial importance for an increase in the reaction yield (high sensitivity) and a decrease in undesirable side reactions, resulting in low photodegradation (high durability). On the other hand, the non-destructive read-out capability is in conflict with the above properties fulfilling conditions (b)–(d). Hence, some external gated-functions are required for the photochromic systems to attain the non-destructive capability while reading the data by the absorption of the light.

Over the years, we reported laser-induced enhancement (> 50 $\times$ ) of the cycloreversion reaction in diarylethene derivatives in solution,<sup>24</sup> polymer films<sup>25</sup> and crystalline phases.<sup>26</sup> The fluence and pulse duration effects of the reaction profiles revealed that higher excited states attained by multiphoton absorption could open effective photochromic reaction channels. In addition, the efficient cycloreversion reaction was also observed in a fulgide derivative<sup>28</sup> in a higher excited state pumped by successive two-photon absorption. This multiphoton-gated reaction may provide an approach to erasable memory media with non-destructive read-out capability in fulgide and diarylethene derivatives. Not only from the viewpoint of the application but also from the basic viewpoints of photochemistry, the selective excitation to a specific electronic state leading to the target reaction seems to provide an important approach for the control of photochemical reactions.

In order to explore the applicability and generality of the multiphoton-gated reaction in 6 $\pi$ -electrocyclic photochromic

<sup>a</sup> Division of Frontier Materials Science, Graduate School of Engineering Science, Center for Quantum Science and Technology under Extreme Conditions, Osaka University, Toyonaka, Osaka, 560-8531, Japan. E-mail: miyasaka@chem.es.osaka-u.ac.jp; Fax: +81-(0)6-6850-6244; Tel: +81-(0)6-6850-6241

<sup>b</sup> CREST, JST, Toyonaka, Osaka, 560-8531, Japan

<sup>c</sup> Department of Applied Chemistry, Graduate School of Engineering, Osaka City University, Sumiyoshi, Osaka, 558-8585, Japan

<sup>d</sup> Department of Chemistry, School of Science, Rikkyo University, Nishi-Ikebukuro, Toshima, Tokyo, 171-8501, Japan

<sup>e</sup> Department of Materials Chemistry, Graduate School of Engineering, Yokohama National University, Tokiwadai, Hodogaya, Yokohama, 240-8501, Japan

compounds, we have investigated the photochromic reaction profiles of three fulgide derivatives under ultrafast laser pulsed excitation in the present work. In the following, we will present the reaction dynamics depending on the pulse duration of the pump laser light sources and the excitation intensity effects of the photochromic reactions.

## Experimental

A picosecond laser photolysis system with a repetitive mode-locked  $\text{Nd}^{3+}:\text{YAG}$  laser was used for transient absorption spectral measurements in the ps–ns time region.<sup>33</sup> The second harmonic (532 nm) with 15 ps excitation pulse was focused into a spot with a diameter of *ca.* 1.5 mm. Picosecond white light continuum generated by focusing a fundamental pulse into a 10 cm quartz cell containing  $\text{D}_2\text{O}-\text{H}_2\text{O}$  (3 : 1) was employed as a monitoring light. A sample cell with 2 mm optical length cell was used. The sample solution was circulated during the measurement under a repetition rate <0.1 Hz and the transient spectrum was obtained with only a one-shot laser exposure. For the measurement of the excitation intensity dependence with the picosecond laser pulse, a pinhole with a diameter of *ca.* 1 mm was placed before the sample solution. The intensity of the picosecond laser light was measured by a laser power meter (Gentec, ED-200).

To investigate the dynamic behaviors under femtosecond laser light excitation, a dual NOPA/OPA laser system was used for transient absorption spectroscopy. The details of the system have been described elsewhere.<sup>24,26–28</sup> Briefly, the output of a femtosecond Ti:Sapphire laser (Tsunami, Spectra-Physics) pumped by the SHG of a cw  $\text{Nd}^{3+}:\text{YVO}_4$  laser (Millennia V, Spectra-Physics) was regeneratively amplified with 1 kHz repetition rate (Spitfire, Spectra-Physics). The amplified pulse (1 mJ pulse<sup>-1</sup> energy, 85 fs fwhm, 1 kHz) was divided into two pulses with the same energy (50%). These fundamental pulses (802 nm) were guided into a non-collinear optical parametric amplifier (NOPA) system (TOPAS-white, Light-Conversion) or an optical parametric amplifier (OPA) system (OPA-800, Spectra-Physics). The NOPA output can cover the wavelength region between 500 and 1000 nm with 1–40 mW output energy with *ca.* 20 fs fwhm. On the other hand, the OPA output pulses are converted to the SHG, THG, FHG, or sum frequency mixing pulse. These pulses can cover the wavelength region between 300 and 1200 nm with 1–10 mW output energy with *ca.* 120 fs fwhm. White light continuum was generated by focusing the fundamental light at 802 nm into a 1 mm quartz window. Polarization of the two pulses was set at the magic angle for all the measurements. The signal and the reference pulses were detected with multichannel diode array systems (PMA-10, Hamamatsu) and sent to a personal computer for further analysis. Spectra were calibrated for group velocity dispersion. From the cross correlation trace at the sample position, the pulse duration of the cross correlation between the NOPA output and the supercontinuum was *ca.* 80 fs for spectra. A rotating sample cell with an optical length of 2 mm was utilized and the absorbance of the sample at the excitation wavelength was set to  $\sim 1.0$ .

Three photochromic fulgide derivatives, 3-isopropylidene-4-[1-(2,5-dimethyl-3-furyl)ethylidene]dihydrofuran-2,5-dione (**F1**),

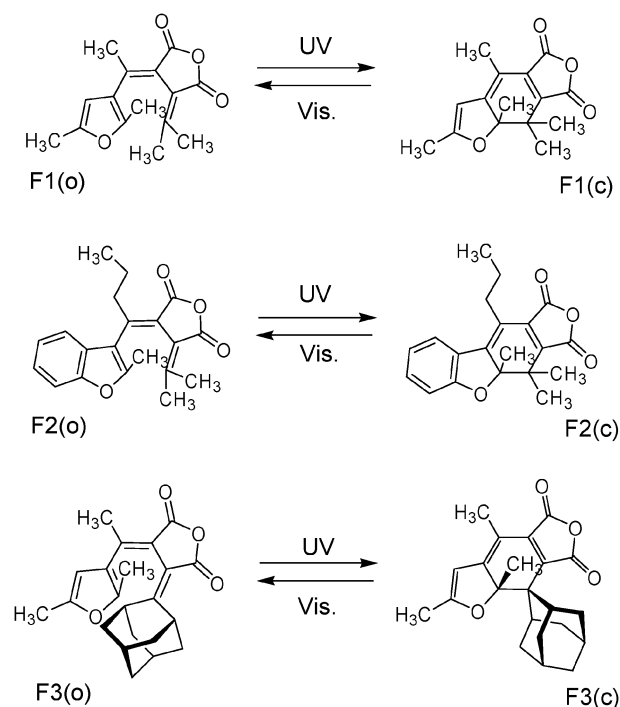
3-isopropylidene-4-[1-(2-methyl-3-benzo[*b*]furyl)butylidene]dihydrofuran-2,5-dione (**F2**) and 3-adamantylidene-4-[1-(2,5-dimethyl-3-furyl)ethylidene]dihydrofuran-2,5-dione (**F3**) were synthesized and purified.<sup>34</sup> Quantum yields of cyclization and cycloreversion were, respectively 0.18 and 0.048 for **F1**, 0.39 and 0.11 for **F2**, and 0.12 and 0.21 for **F3**.<sup>34</sup> Toluene (Wako, infinity pure grade) was used without further purification. All the measurements were performed under  $\text{O}_2$ -free condition at  $22 \pm 2$  °C.

## Results and discussion

### Steady-state absorption spectra

Three fulgide derivatives, **F1**, **F2** and **F3**, undergo photochromic reactions between the open and the closed isomer (*C*-form) as shown in Scheme 1. In general, open forms of the fulgide derivative have two isomers, *E*- and *Z*-forms. Colorless *E*-form can turn to the colored *C*-form in competition with the *cis-trans* isomerization to the colorless *Z*-form upon UV light irradiation, while the *Z*-form does not undergo the cyclization reaction to yield the *C*-form. On the other hand, visible light irradiation of the *C*-form induces the cycloreversion reaction to the *E*-form

Fig. 1 shows the steady-state absorption spectra of the three fulgide derivatives in toluene solution. The dotted line in each of the figures shows the spectrum of the open forms (*E* and *Z* isomers), while the solid line in each of the figures is the spectrum under the photostationary state obtained with 330 nm light irradiation. The closed-forms (*C*-forms) of **F1**, **F2** and **F3**, respectively, have absorption maxima at 494, 475 and 519 nm in the visible region. On the other hand, absorption bands of the open forms of **F1**, **F2** and **F3** are located only in the UV region.



Scheme 1

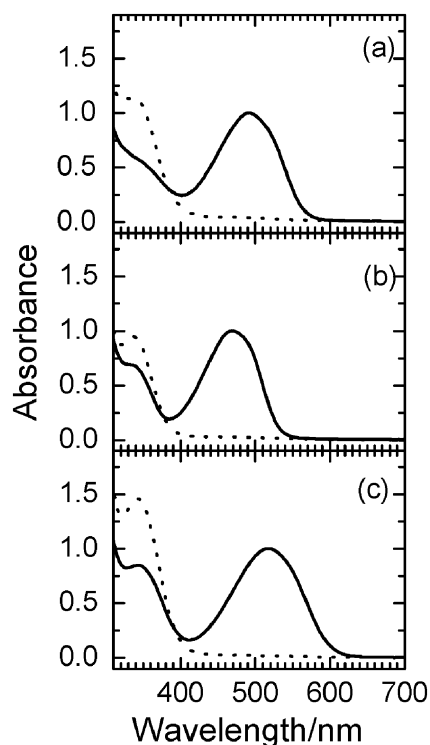


**Fig. 1** Steady-state absorption spectrum of photostationary state of the three fulgide derivatives, (a) **F1**, (b) **F2** and (c) **F3** in toluene solution (solid lines), irradiated at 330 nm. The dotted lines show the open forms (*E*- and *Z*-forms). The main component in the photostationary state is due to the *C*-form.

#### Femtosecond laser photolysis

Fig. 2 shows time-resolved transient absorption spectra of **F1(c)** in toluene solution, excited with a fs laser pulse centered at 510 nm. A negative signal in the wavelength region of 450–525 nm appears within the response function of the apparatus, together with a positive signal at *ca.* 570 nm and a negative one in the wavelength region >620 nm. With increasing delay time, the negative absorbance in the 450–525 nm regions becomes reduced and is followed by a constant negative absorbance. This negative absorbance could be safely assigned to the bleaching of the ground state, because the spectral band shape is similar to the steady-state absorption spectrum of **F1(c)**. On the other hand, the positive signal at *ca.* 570 nm and negative one >620 nm decrease to the baseline with an increase in the delay time after the excitation. The negative signal in the wavelength region >620 nm could be ascribed to the stimulated emission of the excited state of **F1(c)** because the ground state of **F1(c)** has no absorption in this region. In addition, the time constant of the decrease of this negative signal was in agreement with the recovery of the transient bleaching of the ground state, as will be shown in Fig. 3. On the other hand, the positive signal at *ca.* 570 nm could be mainly attributed to the  $S_n \leftarrow S_1$  absorption of **F1(c)** because the decay time constant of this band was almost the same with those of the recovery of the bleaching signal and the stimulated emission. At and after 50 ps following the excitation, no temporal evolution was observed in the transient spectra. In addition, it was confirmed after the fs laser

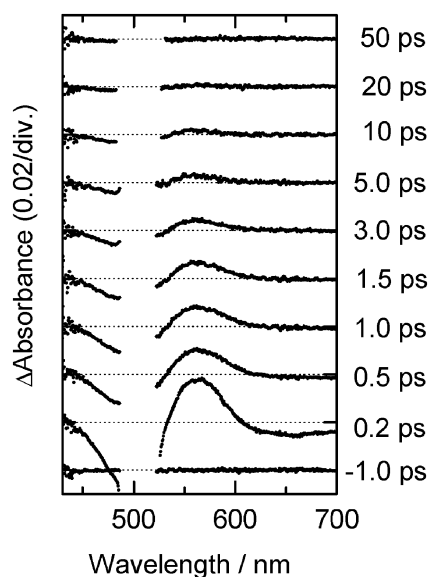


**Fig. 2** Time-resolved transient absorption spectra of the closed form of **F1(c)**, in toluene solution, excited with a *ca.* 20 fs FWHM 510 nm laser pulse with  $2.0 \mu\text{J pulse}^{-1}$  output power. Scattering of excitation light influences the monitoring wavelength region from 490 to 520 nm.

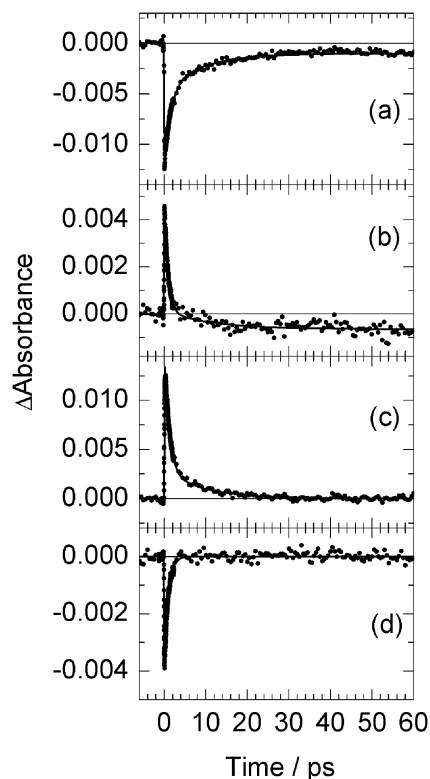


**Fig. 3** Time profiles of transient absorbance of **F1(c)** in toluene solution, excited with a femtosecond 510 nm laser pulse with *ca.* 20 fs FWHM and  $2.0 \mu\text{J pulse}^{-1}$  output power; (a) monitored at 470 nm, (b) 532 nm, (c) 580 nm and (d) 680 nm. Solid black lines are the best calculated curves by taking into account the pulse durations, the time constants, and the reaction yield.

irradiation that the steady-state absorption covering the UV region consisted of only those of the open- and closed-isomers.

UV light irradiation led to perfect recovery of the closed form. From these results, it can be concluded that the cycloreversion reaction was completed within 50 ps following the excitation.

Fig. 3 shows time profiles of **F1(c)** in toluene solution, of which transient absorption spectra were shown in Fig. 2. As was observed in Fig. 2, the time profile at 470 nm shows a quick appearance of the negative absorption due to the transient bleaching of the ground state, followed by the recovery in a few tens of picoseconds. At and after *ca.* 40 ps following the excitation, constant negative absorbance remained. This remaining negative absorbance was attributed to the permanent bleaching due to the cycloreversion reaction, as was explained in the previous section. The time profile was analyzed with the biphasic recovery function with faster and the slower time constants of  $(1.1 \pm 0.1)$  ps and  $(9.5 \pm 1.0)$  ps, respectively. The amplitude factors for the faster, the slower, and the constant negative components are, respectively, 0.62, 0.30 and 0.08. Because the faster time constant is the major component of the ground-state recovery and was in good agreement with the time constant of the stimulated emission at 680 nm, it could be concluded that the time constant of 1.1 ps was due to the lifetime of the excited state. On the other hand, the slower time constant may be attributed to the vibrational cooling in the ground state of the closed-form **F1(c)**. The ground state of **F1(c)** produced immediately after the nonradiative deactivation from the excited state is not thermally relaxed. This hot molecule generally releases its excess energy in a few tens of ps.<sup>35–38</sup>

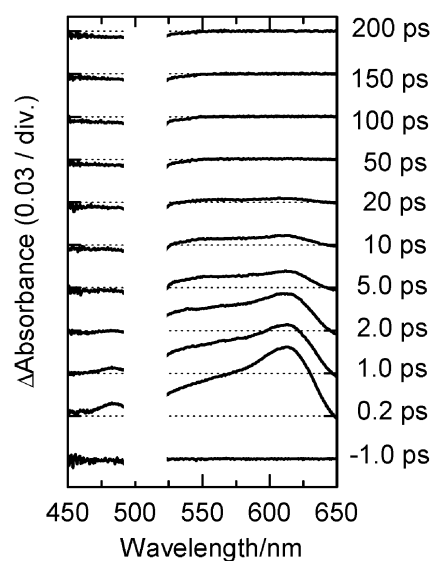
In the time profile monitored at 532 nm in Fig. 3(b), the positive absorbance appearing immediately after the excitation is followed by the decay in a few tens of picoseconds. The positive absorbance immediately after the excitation indicates that the molar absorption coefficient of the excited state at 532 nm is larger than that of the ground state. At and after *ca.* 40 ps following the excitation, a negative constant absorbance was observed. As was explained for Fig. 3(a), this negative absorbance was safely attributed to the cycloreversion reaction. The time profile was analyzed with a biphasic decay function with faster and the slower decay time constants of 1.1 ps and 10.5 ps. The time profile at 580 nm in Fig. 3(c) shows the quick appearance of the positive absorbance, followed by the decay to the baseline in a few tens of picoseconds. The solid line in this figure is the result calculated with the biphasic decay function. The faster and the slower time constants and their amplitude factors were, respectively 1.20 ps, 0.83, and 9.6 ps, 0.17. The faster time constant corresponds to the lifetime of the excited state, indicating that this signal is attributable to the  $S_n \leftarrow S_1$  absorption. On the other hand, the longer decay time constant may be ascribed to the vibrational cooling of the hot  $S_0$  state, because the wavelength at 580 nm is close to the ground-state absorption and the time constant of the decay was similar to those observed in Fig. 3(a) and (b).

The time profile at 680 nm, which could be assigned to the stimulated emission, is exhibited in Fig. 3(d). The decay was reproduced by a single exponential function with a time constant of 1.2 ps. This result supports that the faster time constant observed in Fig. 3(a)–(c) can be assigned to the excited-state lifetime of **F1(c)**. It was confirmed that the

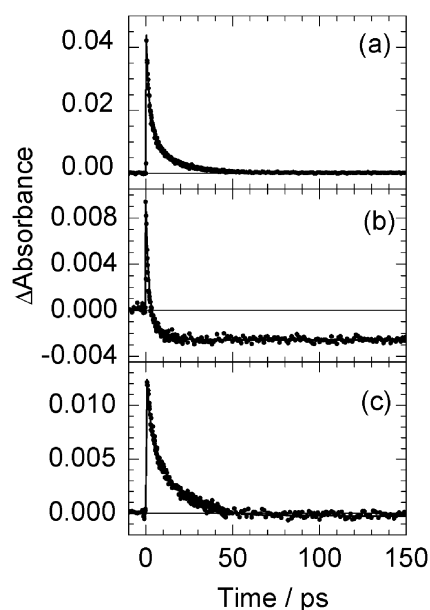
transient absorption spectra and time profiles of Fig. 2 and 3 were independent of the excitation intensity of the femto-second laser pulse with an output of  $1\text{--}3 \mu\text{J pulse}^{-1}$ .

Fig. 4 shows the transient absorption spectra of **F2(c)** in toluene solution, excited with a fs laser pulse centered at 510 nm with *ca.* 20 fs pulse duration. A broad positive band with a maximum at 610 nm appears within the response of the apparatus and decreases to the baseline with an increase in the delay time. This band could be ascribed to the  $S_n \leftarrow S_1$  absorption by the analysis of the time constant in Fig. 5. After the decrease of this band, the negative absorption spectrum with a minimum around 475 nm remains. Since the absorption minimum and spectral band shape of this negative absorption spectrum were identical with those of the ground-state absorption spectrum of **F2(c)**, we can safely attribute this negative transient spectrum to the bleaching of the ground state. At and after 50 ps following the excitation, no temporal evolution was observed in the transient spectra at least up to the time region of a few  $\mu\text{s}$ . In addition, UV-light irradiation to this negative constant absorbance led to perfect recovery to the base line. From these results, it can be concluded that the cycloreversion reaction was completed within 50 ps following the excitation.

Fig. 5 shows time profiles of transient absorbance of **F2(c)** in toluene solution, monitored at several wavelength points. The time profile at 610 nm in Fig. 5(a) shows a quick appearance of the positive signal, which is followed by the decay to the baseline in a few tens of picoseconds. The solid line in this figure is the result calculated on the basis of a biphasic decay with time constants of 1.8 ps and 13.3 ps. Pre-exponential factors for the faster and the slower components were, respectively, 0.58 and 0.42. The faster time constant of 1.8 ps could be ascribed to the lifetime of the excited state of **F2(c)**, because similar time constants were obtained as a major component in other wavelength regions. On the other hand, the slower time constant may be due to the vibrational cooling in the ground state of the closed-form **F2(c)** as mentioned above.



**Fig. 4** Time-resolved transient absorption spectra of the closed-form of **F2(c)**, in toluene solution, excited with *ca.* 20 fs FWHM 510 nm laser pulse with  $2.0 \mu\text{J pulse}^{-1}$  output power. Scattering of excitation light influences the monitoring wavelength region from 490 to 520 nm.



**Fig. 5** Time profiles of transient absorbance of **F2(c)** in toluene solution, excited with a femtosecond 510 nm laser pulse with *ca.* 20 fs FWHM and  $2.0 \mu\text{J pulse}^{-1}$  output power; (a) monitored at 610 nm, (b) 475 nm, and (c) 532 nm. Solid black lines are the best calculated curves by taking into account the pulse durations, the time constants, and the reaction yield.

Fig. 5(b) shows the time profile of the transient absorbance monitored at 475 nm. The positive absorbance in the early stage after the excitation indicates that the molar absorption coefficient of the excited state is larger than that of **F2(c)** in the ground state. The positive absorbance decreased in the initial 10 ps following the excitation and was followed by a constant negative absorbance. This negative constant signal is safely ascribed to the cycloreversion reaction, as was observed in Fig. 4. The time profile was reproduced by a double exponential function with time constants of  $(1.8 \pm 0.2)$  ps and  $(9.5 \pm 1.5)$  ps. Fig. 5(c) shows the time profile monitored at 532 nm, showing the similar time profile as that at 475 nm. The positive absorption appears immediately after the excitation, followed by faster and slower decays with time constants of  $(1.7 \pm 0.15)$  ps and  $(14.0 \pm 1.0)$  ps. Weak permanent negative absorbance remained at and after *ca.* 50 ps, which was due to the cycloreversion process as was observed in Fig. 4. No excitation intensity dependence was observed for the time constants or the ratio of three pre-exponential factors in these time profiles or spectra for excitation intensity of  $1\text{--}3 \mu\text{J pulse}^{-1}$ . These results indicate that the excited state deactivates into the ground state with a time constant of *ca.* 1.8 ps in competition with the cycloreversion reaction.

For **F3(c)**, the transient absorption spectra and time profiles were also observed by means of the same femtosecond laser system. The time constants of these three systems are listed in Table 1.

### Picosecond laser photolysis

Fig. 6 exhibits the time-resolved transient spectra of the three fulgide derivatives, **F1(c)**, **F2(c)** and **F3(c)**, in toluene solution following the picosecond 532 nm laser excitation with

**Table 1** Cycloreversion reaction yields of the three fulgide derivatives in toluene solution and time constants (ps) obtained by transient absorption spectroscopy

	Reaction yield	Transient absorbance		
		Positive signal	Bleaching signal	Stimulated emission
<b>F1</b>	0.048	$1.2 \pm 0.2$ $9.6 \pm 1.0$	$1.1 \pm 0.1$ $9.5 \pm 1.0$	$1.2 \pm 0.2$
<b>F2</b>	0.11	$1.8 \pm 0.2$ $13.3 \pm 0.6$	$1.8 \pm 0.2$ $9.5 \pm 1.5$	—
<b>F3</b>	0.21	$0.7 \pm 0.2$ $9.3 \pm 0.9$	$0.61 \pm 0.1$ $7.0 \pm 1.0$	$0.7 \pm 0.1$

$0.6 \text{ mJ mm}^{-2}$  output power. As stated in the Experimental section, the sample solution was circulated during the measurement under the repetition rate  $< 0.1$  Hz and the data were obtained only with one-shot laser exposure for each spectrum.

Time resolved transient absorption spectra of **F1(c)** in Fig. 6(a) show a negative absorption band around 500 nm and a positive one around 600 nm appearing in the early stage after excitation. The former band is assigned to the bleaching signal of **F1(c)** and the latter is ascribed to the excited state and/or the hot band in the ground state of **F1(c)**, as was explained for Fig. 2. This positive absorption signal decreases to the baseline within 50 ps after the appearance of the pulsed excitation. On the other hand, the bleaching signal slightly recovered also within 50 ps after the excitation. In addition, this negative absorption spectrum was observed even at several seconds after the excitation without circulation of the sample. The UV light irradiation after several hundreds shots of the picosecond laser pulse perfectly recovered the absorbance of **F1(c)**. Hence, the negative absorption spectrum at and after 50 ps was due to the cycloreversion reaction process.

A similar temporal evolution of transient spectra was observed for **F2(c)** and **F3(c)** in Fig. 6(b) and (c). In the early stage after the excitation, the positive bands around 600 nm due to the excited state and thermally unrelaxed ground state of **F2(c)** and **F3(c)** and the bleaching signal around 500 nm appeared. The former positive absorption decreased to the baseline or negative value, while no apparent recovery was observed for the latter bleaching signal and the negative constant value remained at and after 50 ps following the excitation. In both systems, the negative transient spectrum was attributed to the cycloreversion reaction process as for **F1(c)**.

Fig. 7 exhibits the time profiles of closed-forms of **F1**, **F2** and **F3** in toluene solution following picosecond 532 nm laser excitation with  $0.6 \text{ mJ mm}^{-2}$  output power. The time profile at 610 nm of **F1(c)** in Fig. 7(a) shows the positive absorbance appearing within the response of the apparatus, followed by the decay to the baseline in several tens of picoseconds. The solid line in Fig. 7(a) is the curve calculated on the basis of the pulse widths of the exciting and monitoring pulses (15 ps), decay time constants, and amplitude factors obtained by measurements under femtosecond laser exposure. The curve thus calculated reproduces the experimental results well,

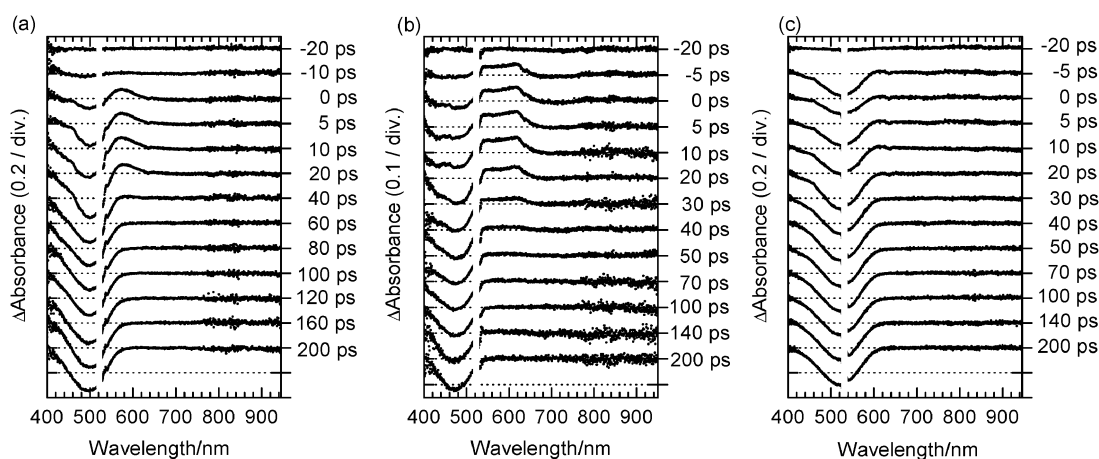


**Fig. 6** Time-resolved transient absorption spectra of three fulgide derivatives in toluene solution, excited with a 15 ps FWHM 532 nm laser pulse with  $0.6 \text{ mJ mm}^{-2}$  output power: (a) **F1(c)**, (b) **F2(c)** and (c) **F3(c)**.

indicating that the time profile obtained by the picosecond laser pulsed excitation is almost the same with that obtained by the femtosecond laser excitation. On the other hand, Fig. 7(b) shows the time profile at 495 nm. The negative absorption appearing within the response of apparatus slightly recovered and attained a negative constant value. This negative absorption signal is due to the cycloreversion process from **F1(c)** to **F1(o)**.

For the analysis of the time profile at 495 nm, we tentatively assumed the simple reaction scheme that the excited state of **F1(c)** undergoes deactivation into the ground state in competition with the cycloreversion reaction leading to the production of **F1(o)**, as shown in Scheme 2. Here, the reaction yield of the cycloreversion,  $\Phi_o$  is represented as  $k_o/(k_n + k_o)$ . Here,  $k_n$  and  $k_o$  are, respectively, the rate constant of the deactivation into the ground state and that of the cycloreversion reaction. In the analysis,  $1/(k_n + k_o)$ , was set to the decay time constant of the positive absorption signals of 1.2 ps, and the relative amplitude factors of the fast and the slow components were set to be the same with those obtained by the femtosecond laser excitation.

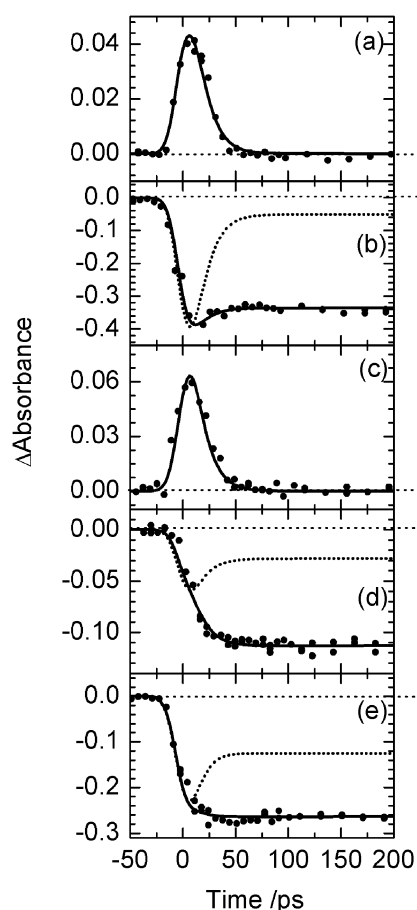
Solid and dotted lines in Fig. 7(b) are the curves calculated with two  $\Phi_o$  values. The dotted line with  $\Phi_o$  value obtained by the steady-state light irradiation, 0.048, does not reproduce the experimental result. On the other hand, the solid line is the result calculated with the  $\Phi_o$  value of 0.60, which reproduces the experimental result. To reproduce the experimental result with no remarkable decay of the negative absorbance, it was revealed that a  $\Phi_o$  value  $\geq 0.6$  was necessary. That is,  $\Phi_o = 0.60$  is the minimum reaction yield estimated by the above procedure. The result in Fig. 7(b) indicates that the cycloreversion reaction is drastically enhanced under the picosecond laser pulse excitation in **F1(c)**, as observed in the diarylethene derivatives<sup>24–27</sup> and a fulgide derivative.<sup>28</sup>

Fig. 7(c) and (d), respectively show time profiles at 610 and 475 nm of **F2(c)** in toluene solution, excited with a picosecond 532 nm laser pulse. As for **F1(c)** in Fig. 7(a), the time profile at 610 nm was reproduced by the curve calculated with the pulse durations and the time constants obtained by the fs laser photolysis. On the other hand, the solid line in Fig. 7(d) is

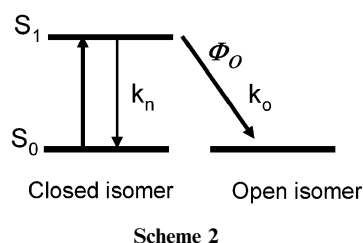
the result calculated on the basis of Scheme 2 with the cycloreversion reaction yield,  $\Phi_o$  of 0.50. The curve thus calculated reproduced the experimental result fairly well, although the quantum yield under steady-state light irradiation was 0.11. This result indicates that the cycloreversion of **F2(c)** was also enhanced by the picosecond 532 nm laser excitation.

Also for **F3(c)** in toluene solution, the same analysis was applied. The time profile at 500 nm in Fig. 7(e) shows the appearance of the negative absorbance within the response function of the apparatus, followed by no remarkable temporal evolution. To reproduce the experimental result within the framework of Scheme 2, an apparent cycloreversion reaction yield  $\geq 0.40$  was required, although the quantum yield under steady-state light irradiation was 0.21. Summarizing the above results and discussion, it can be concluded that these three fulgide derivatives undergo effective cycloreversion reaction under the picosecond 532-nm laser excitation.

To obtain information on the mechanism of this enhancement in the apparent cycloreversion reaction yield, we explored the excitation intensity effect of the cycloreversion reaction. Fig. 8 shows the relation between the excitation intensity and the reaction amount monitored as negative transient absorption signals at 100 ps after the excitation, at which all of the cycloreversion reaction was completed. The ordinate, the conversion efficiency, is the normalized negative absorbance,  $-\Delta A_{\text{max}}(100 \text{ ps})/A_{\text{max}}$ . Here,  $\Delta A_{\text{max}}(100 \text{ ps})$  and  $A_{\text{max}}$  are, respectively the transient absorbance at 100 ps and the ground state absorbance at the wavelength of the absorption maximum of the  $S_1 \leftarrow S_0$  transition in the visible region; 494 nm for **F1(c)**, 475 nm for **F2(c)** and 519 nm for **F3(c)**. Both abscissa and ordinate in Fig. 8 are logarithmic. Each slope in Fig. 8 was 1.5–2.0 in the rather low excitation intensity region, indicating that the cycloreversion reaction is quadratic in proportion with the incident laser intensity. With further increase in the excitation intensity, saturation tendency was observed for all fulgide derivatives. This saturation is partly due to a decreased concentration of the molecules in the ground state in high excitation region, because the maximum value of the ordinate,  $-\Delta A_{\text{max}}(100 \text{ ps})/A_{\text{max}}$  is unity.



**Fig. 7** Time profiles of the transient absorbance of three fulgide derivatives in toluene solution, excited with a 15 ps FWHM, 532 nm laser pulse with  $0.6 \text{ mJ mm}^{-2}$  output power, and observed at two wavelengths where the positive absorption and the bleaching signal occur: (a) at 610 nm and (b) 495 nm for **F1(c)**, (c) at 610 nm and (d) 475 nm for **F2(c)** and (e) at 500 nm for **F3(c)**. Solid and dotted lines are convolution curves calculated with pump and probe pulse widths of 15 ps and double exponential decay-time constants obtained under femtosecond pulse excitation. In this calculation, the reaction yield was set as a parameter. The dotted lines were set to the reaction yields under steady-state light irradiation, while the grey bold lines, with reaction yields of 0.60, 0.50 and 0.40, best reproduce the experimental results in (b), (d) and (e), respectively (see text).



The above results indicate that a two-photon process is responsible for the enhancement of the cycloreversion process under picosecond laser excitation. Usually, two-photon absorption processes can be clarified into two cases such as simultaneous absorption and stepwise absorption.<sup>39</sup> In the former simultaneous absorption process, the ground-state molecule is excited even in the wavelength region where the

molecule has no ground-state absorption. The number of the molecules excited by the simultaneous two-photon absorption is represented by  $N_e = \delta N_g I^2$ . Here,  $\delta$  and  $N_g$  are the two-photon absorption cross-section and the number of the ground state molecules, respectively.  $I$  is the peak intensity of the excitation pulse with the dimension of the number of photons divided by the unit area size and the time. On the other hand, the latter stepwise two-photon absorption process takes place in such a manner that the transient species produced *via* the first one-photon absorption of the ground-state molecule absorbs a second photon, resulting in the production of higher excited states. Since the second photon absorption by the transient species takes place in competition with the first photon absorption by the ground-state molecule, the number of the photons in a laser pulse is an important factor for this stepwise two-photon absorption process.

In the present case, the pulse width and the excitation intensity of the femtosecond laser pulse were *ca.* 1/1000 and 1/100 smaller than those of the picosecond pulse. Hence, the peak intensity of the femtosecond laser pulse,  $I$ , is almost ten times larger than that of the picosecond laser.<sup>40</sup> However, the excitation intensity effect was not observed in the femtosecond laser excitation. These results therefore may lead to the conclusion that the stepwise two-photon absorption is responsible for the drastic enhancement of the cycloreversion reaction in the present systems as observed in diarylethene derivatives<sup>24–27</sup> and a fulgide derivative.<sup>28</sup> However, the lifetime of  $S_1$  state in each fulgide derivative was *ca.* 1/10 shorter than that of the hot molecules and picosecond pulse width. The vibrationally hot molecules in the electronic ground state immediately after the deactivation from the  $S_1$  state may contribute to the drastic enhancement of the cycloreversion reaction *via* second-photon absorption.

In order to more clearly explore the state absorbing the second photon and elucidate the mechanism of nonlinear cycloreversion reaction, we employed two picosecond 532 nm laser pulses for the excitation and investigated the apparent cycloreversion yield as a function of the time interval of these two pulses. Fig. 9(a) shows a schematic illustration of the experimental setup. A 532 nm laser pulse was divided into two pulses with same intensity and one of the two pulses, Pump 2, was guided into the optical delay line to give the time interval,  $\Delta T$ , from the first pulse (Pump 1). The amount of the cycloreversion reaction was monitored as the transient absorption spectrum at 300 ps after the excitation of the second or the first pulse. At a delay time of 300 ps the cycloreversion reaction was completed.

Fig. 9(b) shows the correlation between the transient absorbance of **F1(c)** at 500 nm observed at 300 ps and the time interval between the two pulses,  $\Delta T$ . This correlation curve indicates that the apparent cycloreversion reaction yield has a maximum value at  $\Delta T = 0$  and decreases with an increase in the time interval between the two pulses. The solid line in this figure is the result calculated with the reaction scheme that the intermediate species produced by the first photon absorption is excited again by the second photon absorption leading to the cycloreversion reaction. In this calculation, the lifetime of the intermediate species was varied as a parameter. As clearly shown in this figure, the curve with

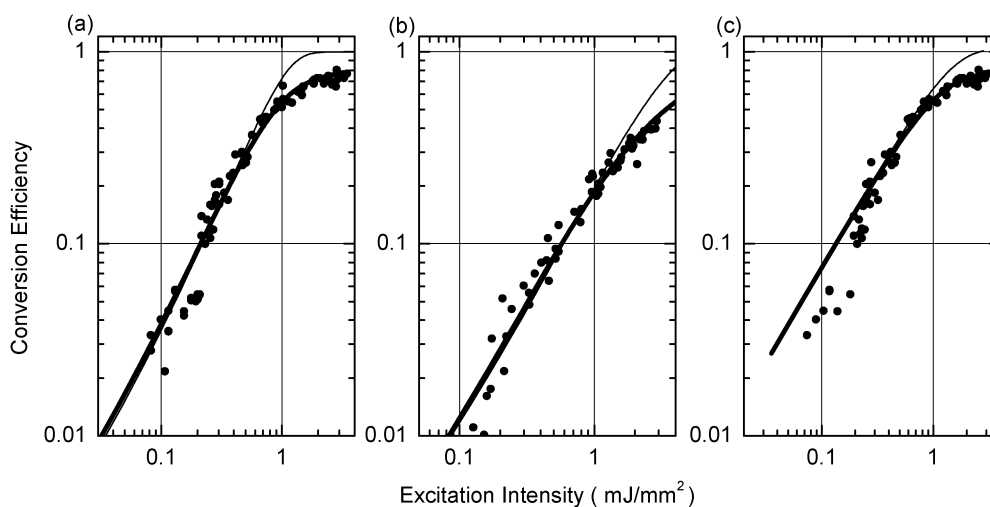


**Fig. 8** Excitation intensity dependence of the conversion efficiency of the three fulgide derivatives in toluene solution, observed at 100 ps after the excitation with a 15 ps FWHM, 532 nm laser pulse (closed circles): (a) **F1(c)**, (b) **F2(c)** and (c) **F3(c)**. Thin and bold black lines in figures are, respectively, the results calculated on the basis of Scheme 3(a) and (b) (see text).

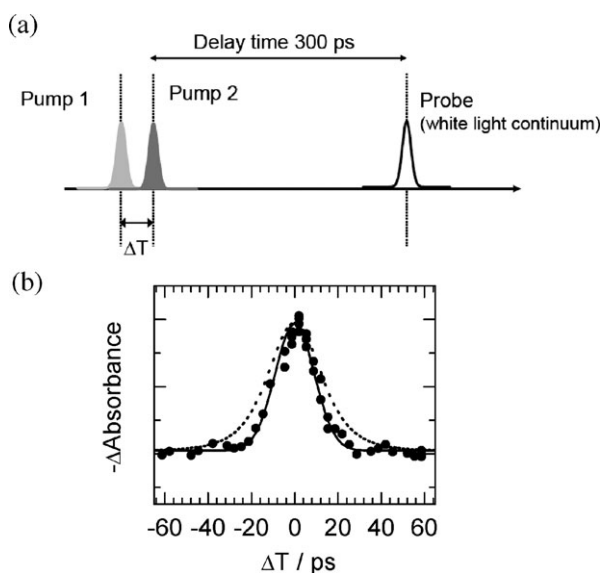
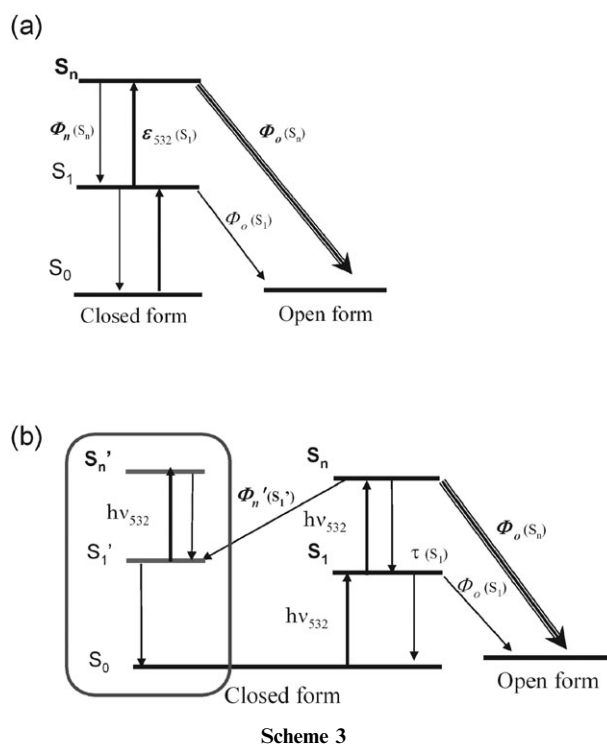


**Fig. 9** (a) Schematic illustration of the double-pulse excitation of ps 532 nm laser light and time monitoring of the cycloreversion reaction. (b) Correlation between the transient absorbance of **F1(c)** monitored at 500 nm (at 300 ps) and the time interval between the two excitation pulses,  $\Delta T$ .

$\tau = 1.0$  ps reproduces the experimental result fairly well but the time constant of 10 ps, which is the time constant of the vibrational cooling, did not reproduce the experimental results. This result clearly indicates that the  $S_1$  state, whose time constant is 1.0 ps, is the main species absorbing the second photon leading to the efficient cycloreversion reaction, and that the hot ground state with a lifetime of 10 ps (vibrational cooling) does not contribute to the efficient cycloreversion. Summarizing the above results and discussion, it can be safely concluded that the stepwise multiphoton absorption *via* the  $S_1$  state prepared by the first photon absorption, such as  $S_0 + h\nu \rightarrow S_1$  and  $S_1 + h\nu \rightarrow S_n \rightarrow$

open-ring form, is responsible also for the enhancement of the cycloreversion reaction of the three fulgide derivatives in toluene solution.

In order to quantitatively obtain the reaction yield in the higher excited state, we applied the numerical simulation<sup>24–28</sup> to the analysis of the results in Fig. 8. Parameters for this simulation are indicated in Scheme 3(a) as italic styles. Here,  $\epsilon_{532}(S_1)$ ,  $\Phi_n(S_n)$  and  $\Phi_o(S_n)$  are, respectively the molar absorption coefficient of the  $S_1$  state at 532 nm, the yield leading to the  $S_1$  state from the higher excited state ( $S_n$ ) attained by the second photon absorption, and the cycloreversion reaction yield at the  $S_n$  state.



In this simulation, the molar absorption coefficient of the  $S_1$  state at 532 nm was experimentally obtained by the analysis of the time profile of transient absorbance monitored at 532 nm after the femtosecond 510 nm laser excitation in the following manner. The time profile of the transient absorbance at 532 nm,  $\Delta A(t)$ , is represented by eqn (1):

$$\Delta A(t) = \left( \varepsilon_{\text{ex}} - \frac{k_n}{k_n + k_o} \varepsilon_g \right) C_{\text{ex}}(t) - \varepsilon_g \frac{k_o}{k_n + k_o} C_{\text{ex}}(0) \quad (1)$$

Here,  $\varepsilon_{\text{ex}}$ ,  $\varepsilon_g$ ,  $k_n$ ,  $k_o$  and  $C_{\text{ex}}(t)$  are, respectively, the molar absorption coefficient of the excited state, that of the ground state, the rate constant of the deactivation into the ground state from the excited state, that of the cycloreversion reaction, and the concentration of the excited state. In this expression, the time profile due to the vibrational cooling was ignored. Since the constant negative absorbance at longer delay times corresponds to the second term of eqn (1), we can acquire  $C_{\text{ex}}(0)$  with the cycloreversion reaction yield obtained by the steady-state irradiation and  $\varepsilon_g$  of the  $S_1 \leftarrow S_0$  absorption at 532 nm. In addition,  $\Delta A(0)$  corresponds to the term,  $(\varepsilon_{\text{ex}} - \varepsilon_g)C_{\text{ex}}(0)$ . Hence, we can estimate the molar absorption coefficient of the excited state at 532 nm, as  $7200 \text{ M}^{-1} \text{ cm}^{-1}$  for **F1(c)**,  $12600 \text{ M}^{-1} \text{ cm}^{-1}$  for **F2(c)**, and  $3600 \text{ M}^{-1} \text{ cm}^{-1}$  for **F3(c)**, respectively. Accordingly, the parameter required for the numerical simulation is only the cycloreversion reaction yield at higher excited state,  $\Phi_o(S_n)$ .

Thin black lines in Fig. 8 are results calculated with  $\Phi_o(S_n)$  of 0.50 for **F1(c)**, 0.55 for **F2(c)** and 0.35 for **F3(c)**, respectively. Although the calculated curves reproduce the experimental result in the region of the excitation intensity  $< ca. 0.7 \text{ mJ mm}^{-2}$ , the deviation between the experimental results and the calculated curve was pronounced with a further increase in the excitation intensity in all systems.

For this deviation, it is worth mentioning that the relaxation from the  $S_n$  state of diarylethene derivative included the internal conversion to the dark electronic state (denoted as  $S_1'$  in Scheme 3(b)) in addition to the cycloreversion reaction and the relaxation to the  $S_1$  state.<sup>24–26</sup> This  $S_1'$  species was assigned to the excited state which is located in the vicinity of the  $S_1$  state but optically forbidden from the  $S_0$  state.<sup>24–26</sup> In addition, it was revealed that this species did not undergo efficient cycloreversion even if it was pumped up into higher excited state by the second photon absorption.

For the analysis of the present fulgide systems, we included this  $S_1'$  state in the analysis. The lifetime of this  $S_1'$  state,  $\tau(S_1')$ , was varied to reproduce the experimental results. Bold black lines in Fig. 8 are the results calculated with the cycloreversion reaction yield in the  $S_n$  state of 0.50 for **F1(c)**, 0.55 for **F2(c)** and 0.35 for **F3(c)**, and  $\tau(S_1')$  of 11 ps, showing that the experimental results are well reproduced by the calculated results. The iterative simulation estimated the reaction yield in the higher excited state was estimated at  $0.50 \pm 0.05$  for **F1(c)**,  $0.55 \pm 0.05$  for **F2(c)** and  $0.35 \pm 0.05$  for **F3(c)**. Summarizing the above results and discussion, it can be concluded that the stepwise two-photon process *via* the actual intermediate  $S_1$  state, rather than the simultaneous two-photon process, was responsible for the enhancement of the cycloreversion process of the three fulgide derivatives under the picosecond laser excitation. The production of the  $S_n$  state

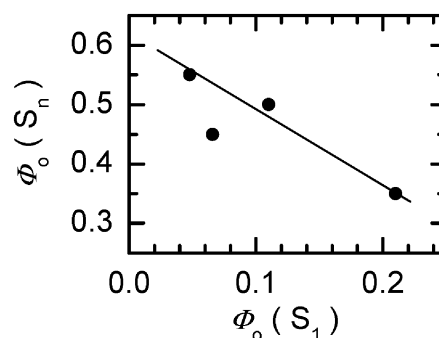


**Fig. 10** Relation between the reaction yields of  $\Phi_o(S_1)$  and  $\Phi_o(S_n)$  in fulgide derivatives. The previous result of another fulgide system (0.066 for  $\Phi_o(S_1)$  and 0.45 for  $\Phi_o(S_n)$ ) is also given.<sup>28</sup> The solid line is to guide the eye.

with high reaction yields plays an important role in the enhancement of the cycloreversion reaction, as observed for diarylethene derivatives<sup>24–26</sup> and a fulgide derivative.<sup>28</sup> As a result, the generality of the multiphoton-gated process in the system with the heterocyclic aryl groups was confirmed.

Finally, it is noteworthy that for **F3(c)**, with the largest  $\Phi_o(S_1)$  among the present three fulgide derivatives, has the smallest cycloreversion reaction yield for  $\Phi_o(S_n)$ , as shown in Fig. 10, where the previous results of a further fulgide system<sup>28</sup> are also given. This tendency was also observed in diarylethene derivatives. For example, while a diarylethene derivative with a lower  $\Phi_o(S_1)$  of 1.3% has a higher reactivity of the higher excited state,<sup>24</sup> another derivative with  $\Phi_o(S_1) = 35\%$  does not.<sup>27a</sup> These results imply that the character of higher electronic state attained by the second photon absorption from the  $S_1$  state plays an important role for the efficient cycloreversion. That is, the  $S_1$  molecular electronic wave function feasible for the cycloreversion in the  $S_1$  state is not feasible for the efficient reaction by the optical allowed transition. At any rate, the present results suggest that the two-photon gated cycloreversion is an effective method for actual application, since it is effective for molecular systems with low reaction yield in the  $S_1$  state. We are presently undertaking the investigation of the relation between cycloreversion reaction yield in higher excited states under stepwise excitation and under one-photon excitation, the results of which will be reported soon.

## Conclusion

Cycloreversion processes of three photochromic fulgide derivatives in toluene solution were investigated by means of picosecond and femtosecond laser spectroscopy. The bond fission occurred within a few picoseconds. Picosecond pulsed excitation of the closed-isomer of the diarylethene derivatives led to the drastic enhancement of the cycloreversion reaction. The dependence of the reaction profiles on the excitation intensity, pulse duration, and the excitation wavelength indicated that this enhancement is attributable to the production of the higher excited state with a large reaction yield of the cycloreversion attained *via* a successive two-photon process. This process generally occurred in fulgide derivatives as well as diarylethene derivatives and the generality of the stepwise

two-photon process was confirmed for the  $6\pi$ -electrocyclic photochromic compounds. The correlation of the reaction yield in the  $S_1$  state with that in  $S_n$  states suggest the character of the electronic states connected by the optical absorption plays an important role in the control of the cycloreversion reaction.

## Acknowledgements

This work was partly supported by Grand-in-Aids for Research in Priority Area (No. 471) from the Ministry of Education, Culture, Sports, Science, and Technology (MEXT) of the Japanese Government.

## References

- (a) *Photochromism Molecules and Systems*, ed. H. Dürr, H. Bouas-Laurent, Elsevier, Amsterdam, 1990; (b) *Photochromism*, ed. C. H. Brown, Wiley-Interscience, New York, 1971.
- (a) *Molecular Switches*, ed. B. L. Feringa, Wiley-VCH, Weinheim, 2001; (b) Thematic issue on "Photochromism, Memories and Switches", *Chem. Rev.*, 2000, **100**, whole of issue 5; (c) *Photo-reactive Materials for Ultra-high Density Optical Memory*, ed. M. Irie, Elsevier, Amsterdam, 1994; (d) S. Kobatake and M. Irie, *Annu. Rep. Prog. Chem., Sect. C: Phys. Chem.*, 2003, **99**, 277.
- (a) M. Irie, *Chem. Rev.*, 2000, **100**, 1685; (b) M. Irie and K. Uchida, *Bull. Chem. Soc. Jpn.*, 1998, **71**, 985.
- (a) S. Kobatake and M. Irie, *Bull. Chem. Soc. Jpn.*, 2004, **77**, 195; (b) K. Matsuda and M. Irie, *Chem. Lett.*, 2006, **35**, 1204; (c) M. Irie, *Bull. Chem. Soc. Jpn.*, 2008, **81**, 917.
- (a) H. G. Heller, *Spec. Publ., R. Soc. Chem., Fine Chem. Electron. Ind.*, 1986, **60**, 120; (b) J. Whittall, Fulgides and Fulgimides—A Promising Class of Photochrome for Application, in *Applied Photochromic Polymer Systems*, ed. C. B. McArdle, Blackie, Glasgow, 1992, ch. 3, p. 80; (c) M. Fan, L. Yu and W. Zhao, Fulgide Family Compounds: Synthesis, Photochromism, and Applications, in *Organic Photochromic and Thermochromic Compounds, Vol. 1, Main Photochromic Families*, ed. J. C. Crano, R. Guglielmetti, Plenum Publishers, New York, 1999, ch. 4, p. 141.
- Y. Yokoyama, *Chem. Rev.*, 2000, **100**, 1717.
- (a) A. Fernandez-Acebes and J.-M. Lehn, *Chem.-Eur. J.*, 1999, **5**, 3285; (b) G. M. Tsvigoulis and J.-M. Lehn, *Angew. Chem., Int. Ed. Engl.*, 1995, **34**, 1119; (c) S. L. Gilat, S. Kawai and J.-M. Lehn, *J. Chem. Soc., Chem. Commun.*, 1993, 1439.
- (a) L. N. Lucas, J. J. D. de Jong, J. H. van Esch, R. M. Kellogg and B. L. Feringa, *Eur. J. Org. Chem.*, 2003, 155; (b) B. L. Feringa, W. F. Jager and B. Delange, *Tetrahedron*, 1993, **49**, 8267; (c) B. L. Feringa, *J. Org. Chem.*, 2007, **72**, 6635.
- (a) A. Peters and N. R. Branda, *J. Am. Chem. Soc.*, 2003, **125**, 3404; (b) A. J. Myles and N. R. Branda, *Adv. Funct. Mater.*, 2002, **12**, 167; (c) E. Murguly, T. B. Norsten and N. R. Branda, *Angew. Chem., Int. Ed.*, 2001, **40**, 1752.
- (a) Q. Luo, B. Chen, M. Wang and H. Tian, *Adv. Funct. Mater.*, 2003, **13**, 233; (b) Y. Yokoyama, H. Shiraishi, Y. Tani, Y. Yokoyama and Y. Yamaguchi, *J. Am. Chem. Soc.*, 2003, **125**, 7194; (c) K. Uchida, M. Saito, A. Murakami, S. Nakamura and M. Irie, *ChemPhysChem*, 2003, **4**, 1124.
- (a) M. Irie, T. Fukaminato, T. Sasaki, N. Tamai and T. Kawai, *Nature*, 2002, **420**, 759; (b) T. Kawai, T. Sasaki and M. Irie, *Chem. Commun.*, 2001, 711; (c) T. B. Norsten and N. R. Branda, *J. Am. Chem. Soc.*, 2001, **123**, 1784.
- (a) J. Chauvin, T. Kawai and M. Irie, *Jpn. J. Appl. Phys.*, 2001, **40**, 2518; (b) T. Kawai, N. Fukuda, D. Gröschl, S. Kobatake and M. Irie, *Jpn. J. Appl. Phys.*, 1999, **38**, L1194.
- (a) S. L. Gilat, S. H. Kawai and J.-M. Lehn, *Chem.-Eur. J.*, 1995, **1**, 275; (b) T. Kawai, T. Kunitake and M. Irie, *Chem. Lett.*, 1999, 905.
- (a) S. Yamamoto, K. Matsuda and M. Irie, *Angew. Chem., Int. Ed.*, 2003, **42**, 1636; (b) T. Kodani, K. Matsuda, T. Yamada, S. Kobatake and M. Irie, *J. Am. Chem. Soc.*, 2000, **122**, 9631; (c) T. Yamaguchi, K. Uchida and M. Irie, *J. Am. Chem. Soc.*, 1997, **119**, 6066.
- (a) L. Khedhiri, A. Corval, R. Casalegno and M. Rzaigui, *J. Phys. Chem. A*, 2004, **108**, 7473; (b) J. Harada, R. Nakajima and K. Ogawa, *J. Am. Chem. Soc.*, 2008, **130**, 7085.
- (a) M. Morimoto, S. Kobatake and M. Irie, *Chem. Rec.*, 2004, **4**, 23; (b) S. Kobatake and M. Irie, *Bull. Chem. Soc. Jpn.*, 2004, **77**, 195; (c) M. Irie, S. Kobatake and M. Horichi, *Science*, 2001, **291**, 1769; (d) M. Irie, T. Lifka, S. Kobatake and N. Kato, *J. Am. Chem. Soc.*, 2000, **122**, 4871; (e) S. Kobatake, T. Yamada, K. Uchida, N. Kato and M. Irie, *J. Am. Chem. Soc.*, 1999, **121**, 2380.
- S. Kobatake, S. Takami, H. Mito, T. Ishikawa and M. Irie, *Nature*, 2007, **446**, 778.
- N. Tamai and H. Miyasaka, *Chem. Rev.*, 2000, **100**, 1875.
- (a) H. D. Ilge, M. Kaschke and D. Khechinashvili, *J. Photochem.*, 1986, **33**, 349; (b) S. Kurita, A. Kashiwagi, Y. Kurita, H. Miyasaka and N. Mataga, *Chem. Phys. Lett.*, 1990, **171**, 553.
- (a) F. O. Koller, W. J. Schreier, T. E. Schrader, A. Sieg, S. Malkmus, C. Schulz, S. Dietrich, K. Ruck-Braun, W. Zinth and M. Braun, *J. Phys. Chem. A*, 2006, **110**, 12769; (b) S. Malkmus, F. O. Koller, B. Heinz, W. J. Schreier, T. E. Schrader, W. Zinth, C. Schulz, S. Dietrich, K. Ruück-Braun and M. Braun, *Chem. Phys. Lett.*, 2006, **417**, 266; (c) B. Heinz, S. Malkmus, S. Laimgruber, S. Dietrich, C. Schulz, K. Rück-Braun, M. Braun, W. Zinth and P. Gilch, *J. Am. Chem. Soc.*, 2007, **129**, 8577.
- T. Cordes, S. Malkmus, J. A. DiGirolamo, W. J. Lees, A. Nenov, R. de Vivie-Riedle, M. Braun and W. Zinth, *J. Phys. Chem. A*, 2008, **112**, 13364.
- S. C. Martin, N. Singh and S. C. Wallace, *J. Phys. Chem.*, 1996, **100**, 8066.
- (a) H. Miyasaka, S. Araki, A. Tabata, T. Nobuto, N. Mataga and M. Irie, *Chem. Phys. Lett.*, 1994, **230**, 249; (b) H. Miyasaka, T. Nobuto, A. Itaya, N. Tamai and M. Irie, *Chem. Phys. Lett.*, 1997, **269**, 281; (c) H. Miyasaka, T. Nobuto, M. Murakami, A. Itaya, N. Tamai and M. Irie, *J. Phys. Chem. A*, 2002, **106**, 8096; (d) T. Kaieda, S. Kobatake, H. Miyasaka, M. Murakami, N. Iwai, N. Nagata, A. Itaya and M. Irie, *J. Am. Chem. Soc.*, 2002, **124**, 2015.
- (a) H. Miyasaka, M. Murakami, A. Itaya, D. Guillaumont, S. Nakamura and M. Irie, *J. Am. Chem. Soc.*, 2001, **123**, 753; (b) M. Murakami, H. Miyasaka, T. Okada, S. Kobatake and M. Irie, *J. Am. Chem. Soc.*, 2004, **126**, 14764.
- S. Ryo, Y. Ishibashi, M. Murakami, H. Miyasaka, S. Kobatake and M. Irie, *J. Phys. Org. Chem.*, 2007, **20**, 953.
- (a) Y. Ishibashi, K. Tani, H. Miyasaka, S. Kobatake and M. Irie, *Chem. Phys. Lett.*, 2007, **437**, 243; (b) K. Tani, Y. Ishibashi, H. Miyasaka, S. Kobatake and M. Irie, *J. Phys. Chem. C*, 2008, **112**, 11150.
- (a) H. Miyasaka, M. Murakami, T. Okada, Y. Nagata, A. Itaya, S. Kobatake and M. Irie, *Chem. Phys. Lett.*, 2003, **371**, 40; (b) K. Uchida, A. Takata, S. Ryo, M. Saito, M. Murakami, Y. Ishibashi, M. Miyasaka and M. Irie, *J. Mater. Chem.*, 2005, **15**, 2128.
- Y. Ishibashi, M. Murakami, H. Miyasaka, S. Kobatake, M. Irie and Y. Yokoyama, *J. Phys. Chem. C*, 2007, **111**, 2730.
- N. Tamai, T. Saika, T. Shimidzu and M. Irie, *J. Phys. Chem.*, 1996, **100**, 4689.
- (a) J. Ern, A. T. Bens, A. Bock, H.-D. Martin and C. Kryschi, *J. Lumin.*, 1998, **76/77**, 90; (b) J. Ern, A. T. Bens, H.-D. Martin, S. Mukamel, D. Schmid, S. Tretiak, E. Tspier and C. Kryschi, *Chem. Phys.*, 1999, **246**, 115; (c) J. Ern, A. T. Bens, H.-D. Martin, S. Mukamel, S. Tretiak, K. Tsyganenko, K. Kuldova, H. P. Trommsdorff and C. Kryschi, *J. Phys. Chem. A*, 2001, **105**, 1741; (d) J. Ern, A. T. Bens, H.-D. Martin, K. Kuldova, H. P. Trommsdorff and C. Kryschi, *J. Phys. Chem. A*, 2002, **106**, 1654.
- (a) P. R. Hania, R. Telesca, L.N. Lucas, A. Pugzlys, J. van Esch, B. L. Feringa, J. G. Snijders and K. Duppen, *J. Phys. Chem. A*, 2002, **106**, 8498; (b) P. R. Hania, A. Pugzlys, L. N. Lucas, J. J. D. de Jong, B. L. Feringa, J. H. van Esch, H. T. Jonkman and K. Duppen, *J. Phys. Chem. A*, 2005, **109**, 9437.
- (a) S. Shim, T. Joo, S. C. Bae, K. S. Kim and E. Kim, *J. Phys. Chem. A*, 2003, **107**, 8106; (b) S. Shim, I. Eom, T. Joo, E. Kim and K. S. Kim, *J. Phys. Chem. A*, 2007, **111**, 8910.

- 33 (a) H. Miyasaka, T. Moriyama, S. Kotani, R. Muneyasu and A. Itaya, *Chem. Phys. Lett.*, 1994, **225**, 315; (b) H. Miyasaka, T. Moriyama and A. Itaya, *J. Phys. Chem.*, 1996, **100**, 12609.
- 34 (a) Y. Yokoyama, T. Goto, T. Inoue, M. Yokoyama and Y. Kurita, *Chem. Lett.*, 1988, 1049; (b) Y. Yokoyama, T. Inoue, M. Yokoyama, T. Goto, T. Iwai, N. Kera, I. Hitomi and Y. Kurita, *Bull. Chem. Soc. Jpn.*, 1994, **67**, 3297.
- 35 A. Seilmeier and W. Kaiser, in *Ultrashort laser pulses and applications*, ed. W. Kaiser, Springer, Berlin, 1988, p. 279.
- 36 B. I. Greene, R. M. Hochstrasser and R. B. Weisman, *J. Chem. Phys.*, 1979, **71**, 1247.
- 37 (a) H. Miyasaka, H. Masuhara and N. Mataga, *Laser Chem.*, 1983, **1**, 357; (b) H. Miyasaka, M. Hagihara, T. Okada and N. Mataga, *Chem. Phys. Lett.*, 1992, **188**, 259.
- 38 K. Iwata and H. Hamaguchi, *J. Phys. Chem. A*, 1997, **101**, 632.
- 39 (a) L. R. Sutherland, *Handbook of Nonlinear Optics*, Marcel Dekker, Inc., New York, 2nd edn, 2003; (b) S. Kershaw, Two-Photon Absorption, in *Characterization Techniques and Tabulations for Organic Nonlinear Optical Materials*, ed. M. G. Kuzyk, C. W. Dirk, Marcel Dekker, Inc., New York, 1998, ch. 7.
- 40 The output of  $1 \text{ mJ mm}^{-2}$  of the picosecond laser pulse at 532 nm with 15 ps fwhm corresponds to  $I$  of  $1.79 \times 10^{28}$  photons  $\text{cm}^{-2} \text{s}^{-1}$ . The value of  $N_g$  is  $6.02 \times 10^{16}$  molecules  $\text{cm}^{-3}$  for  $1 \times 10^{-4}$  M concentration. By using the typical value of the two-photon absorption cross-section,  $10^{-50} \text{ cm}^4 \text{ s (photon molecule)}^{-1}$ ,<sup>39</sup> the level of excited state molecules produced by the above  $I$  value is estimated to be  $2.87 \times 10^{12}$  molecules  $\text{cm}^{-3}$  or  $4.78 \times 10^{-9}$  M. This estimation indicates that the simultaneous two-photon absorption is rather difficult for the present excitation conditions of the picosecond laser pulse.